DOI: 10.1002/cphc.201000306

Photostimulated Reduction Processes in a Titania Hybrid Metal–Organic Framework

Aron Walsh* and C. Richard A. Catlow[a]

Titanium dioxide is the most widely studied photocatalytic metal oxide system, owing largely to the facile chemical reduction of Ti^{IV} to Ti^{III}, which can act as catalytic redox centres,[1] and the early demonstration of its ability to dissociate water into gaseous hydrogen and oxygen under ultraviolet (UV) illumination.[2,3] Tailoring of the electronic properties of TiO_2 is generally performed by chemical doping or alloying,[4,5] or through the absorption of organic moieties on the surface, as in dye-sensitized solar cells.[6,7] The formation of hybrid inorganic–organic solids, containing metal oxide networks of reduced dimensionality, offers a new pathway for material functionalization including chemical engineering of optoelectronic properties.[8–11]

Synthesis of a photoactive hybrid solid derived from titania was recently reported by Dan-Hardi et al.:[12] the porous structure is composed of octameric rings of Ti–O polyhedra connected by aromatic dicarboxylate linkers, as shown in Figure 1. While the large internal surface area (1550 $m^2 g^{-1}$) offers potential for gas storage and steric-selective catalysis, most intriguing are its properties under illumination, resulting in a reversible photochromic transition from white to dark blue on irradiation under UV light, which has been assigned to the occurrence of new absorption bands at 2.10 and 2.47 eV. Electron spin resonance spectra indicated the formation of Ti^{III} species, but the route to their formation is so far unclear. In bulk TiO_2, localized Ti reductions are generally attributed to a combination of oxygen vacancy formation and titanium interstitials.[13,14]

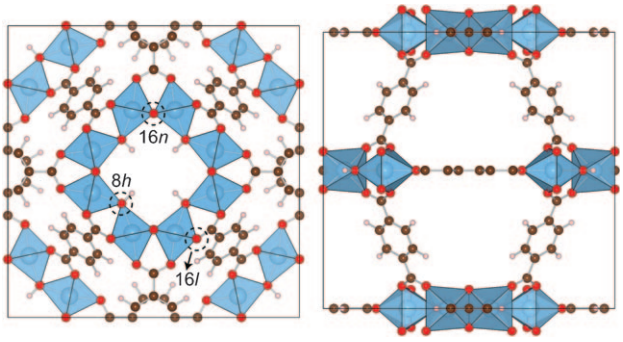

Figure 1. The tetragonal crystal structure of titanium carboxylate viewed along the [001] (left) and [100] (right) directions. The oxygen atoms are coloured red, with brown = carbon, pink = oxygen, and blue = titanium; the three inequivalent oxygen sites are indicated by their Wyckoff positions.

By examining the electronic and defect structure of the hybrid titania system, using quantum chemical simulations, we propose the origin of its remarkable photochromic properties: optical excitations larger than the band gap will result in reduced titanium centres, which introduce new states in the electronic gap; charge compensation can be achieved either through the loss of oxygen or hydroxyl formation. In contrast to the parent inorganic system, in the hybrid material, direct self-compensation of reducing defects can be achieved owing to the chemical flexibility of the organic framework, and the spatial separation of electrons and holes is confirmed between the inorganic and organic sub-networks.

The tetragonal ($\bar{I}42$) crystal structure of titanium carboxylate has been determined by X-ray powder diffraction.[12] Electronic structure calculations were performed on the 240 atom unit cell ($C_{96}H_{56}O_{72}Ti_{16}$) using density functional theory (DFT),[15,16] with the semi-local PBE[17] exchange-correlation functional. To account for the DFT electron self-interaction error, additional calculations were performed using an on-site Coulomb correction (PBE + U):[18] a typical value of 5 eV was applied to the Ti d orbitals, which has been optimised to describe the Ti^{IV} to (III) reaction;[13,14] the 3d orbitals are formally *unoccupied*, and therefore the correction becomes largest when the system is chemically reduced. A plane wave expansion up to 500 eV was used to form the well-converged basis set, while k-point sampling was performed at the Brillouin zone centre, with the exception of the density of states calculations, which were performed using a 3×3×3 Monkhorst–Pack[19] k-point mesh.

Relaxation of the cell vectors, angles and internal positions (to within 0.01 eV $Å^{-1}$) at both the PBE and PBE + U levels produced equilibrium structural parameters within 3% of experimental room temperature values (see Table 1). At the PBE + U

Table 1. Calculated equilibrium structural parameters and band gap of titanium dicarboxylate at the PBE and PBE + U levels of DFT. Percentage errors with respect to room-temperature diffraction data are given in brackets.

	GGA	GGA + U	Experiment[12]
a [Å]	19.08 (+2.31%)	19.21 (+3.00%)	18.65
b [Å]	19.08 (+2.31%)	19.21 (+3.00%)	18.65
c [Å]	18.13 (−0.01%)	18.19 (+0.28%)	18.14
Ti–O [Å]	2×2.07	2.09	1.98
	2×2.05	2.08	1.94
	2×1.85	1.89	1.89
E_g [eV]	2.87	3.14	

[a] *Dr. A. Walsh, Prof. C. R. A. Catlow*
University College London, Department of Chemistry
Materials Chemistry, Third Floor, Kathleen Lonsdale Building
Gower Street, London WC1E 6BT (UK)
Fax: (+44) 02076790493
E-mail: a.walsh@ucl.ac.uk

 © 2010 Wiley-VCH Verlag GmbH & Co. KGaA, Weinheim

level of theory, the titania polyhedra are mildly expanded with an increase in volume of the Ti–O octahedra from 10.40 to 10.81 Å^3. The calculated electronic band gap is 2.9–3.1 eV, and given that the typical band gap underestimation of semi-local DFT functionals for TiO_2 is of the order of 1 eV, we expect that the experimental gap would lie in the UV range at around 4 eV (neglecting excitonic effects), consistent with its lack of colouration.[12]

The occupied electronic density of states, in the upper valence band, consist of a mixture of C and O 2*p* states, with some lesser contributions from Ti and H, as shown in Figure 2.

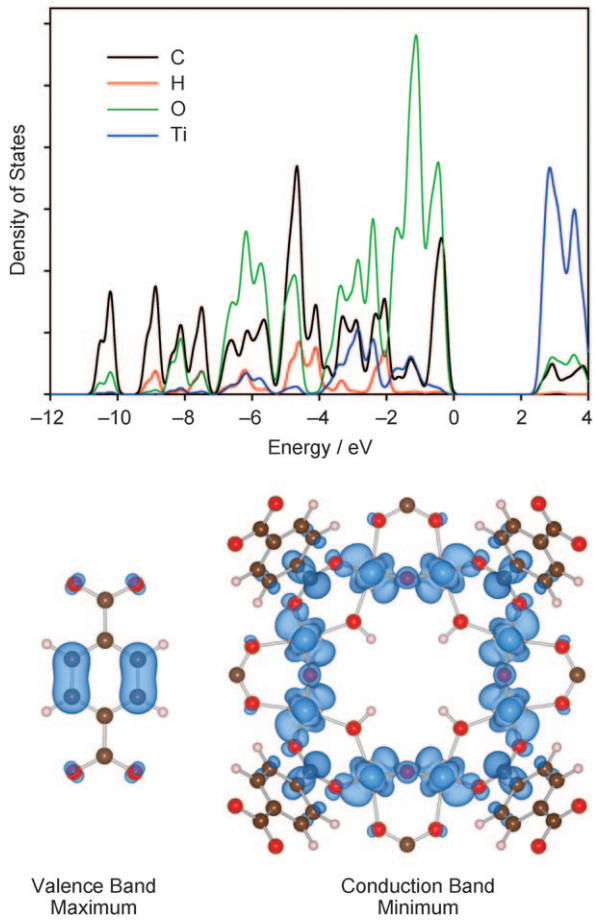

Figure 2. Electronic density of states and the density isosurface associated with the band edge states of bulk titanium carboxylate calculated using the PBE density functional. The highest occupied states are localized on the aromatic organic group, while the lowest unoccupied states are localized on the octameric TiO_2 units.

Importantly, in contrast to bulk TiO_2, where the top of the valence band is strongly localized on oxygen, here it is the π orbitals of the aromatic linking groups which contribute to the highest occupied states. The conduction band network is centred on the octameric TiO_2 units (Ti *d*–O *p* hybridized orbitals), which indicates that the lowest energy optical excitations across the band edges will involve transitions between the organic and inorganic sub-networks.

Two direct routes for chemical reduction could be envisaged in the hybrid material: oxygen vacancy formation to release gaseous oxygen [shown using the standard notation of Kröger and Vink, see Eq. (1)]:

$$2\,Ti_{Ti} + O_O \rightleftharpoons V_O^{\bullet\bullet} + 2\,Ti_{Ti}^{/} + \frac{1}{2}\,O_2 \qquad (1)$$

and hydroxyl formation at the exposed oxygen 16*n* position in the octameric TiO_2 ring centre [Eq. (2)]:

$$Ti_{Ti} + O_O + \frac{1}{2}\,H_2 \rightleftharpoons (OH)_O^{\bullet} + Ti_{Ti}^{/} \qquad (2)$$

Both reduction mechanisms are considered to be electronically compensated through localized titanium reduction from Ti^{4+} to Ti^{3+}, that is [Eq. (3)]:

$$Ti_{Ti}^{x} + e^{/} \rightleftharpoons Ti_{Ti}^{/} \qquad (3)$$

For vacancy formation, there are the three inequivalent oxygen atoms illustrated in Figure 1: the 16*n* Wyckoff site (an edge sharing position between two Ti octahedra); the 8*h* site (a corner sharing hydroxyl group); the 16*l* site (a bridging carboxylate oxygen). For the 16*n* case, oxygen vacancy formation results in the occupation of two quasiatomic Ti d_{xz} orbitals neighbouring the vacancy in a triplet spin configuration; at the PBE+*U* level, the states are more localized on the neighbouring Ti ions as shown in Figure 3, and form a distinct split off state in the band gap, similar to reduced TiO_2 surfaces[20] and intrinsic defects in bulk TiO_2.[13,14] The defect reaction energy at the PBE level of 3.66 eV is reduced to 2.72 eV when the self interaction of the electrons is addressed; this large difference is due to the significant reduction in energy of the single-particle defect state at the PBE+*U* level. In comparison, the calculated oxygen vacancy energy in bulk TiO_2 is 4 eV at the same level of theory,[14] indicating that the process will occur more readily in the hybrid material system.

Removal of the 8*h* and 16*l* oxygen atoms results in a different behaviour with *no* excess electrons produced: the first vacancy is compensated by the remaining hydrogen, which becomes anionic [H^-, Eq. (4)]:

$$OH_{OH} \rightleftharpoons H_{OH}^{x} + \frac{1}{2}\,O_2 \qquad (4)$$

while the second is compensated by the formation of a direct C–Ti bond, that is, $[C{-}O{-}Ti]^x \rightarrow [C{-}Ti]^x$. Both defect reactions maintain the insulating band gap of the host material, and the reaction energies are significantly higher than the formation of an oxygen vacancy compensated by titanium reduction, as listed in Table 2.

Let us now consider Equation (2) and specifically the incorporation of an additional H atom to form an hydroxyl group with the exposed 16*n* oxygen in the ring centre. The calculations predict that the reaction is exothermic by as much as 0.6 eV, which is consistent with the strong reducing behaviour of H_2; however, it should be recognized that finite temperature effects and the activation barrier for dissociation have not been addressed here. The end result of hydrogen incorpora-

 © 2010 Wiley-VCH Verlag GmbH & Co. KGaA, Weinheim

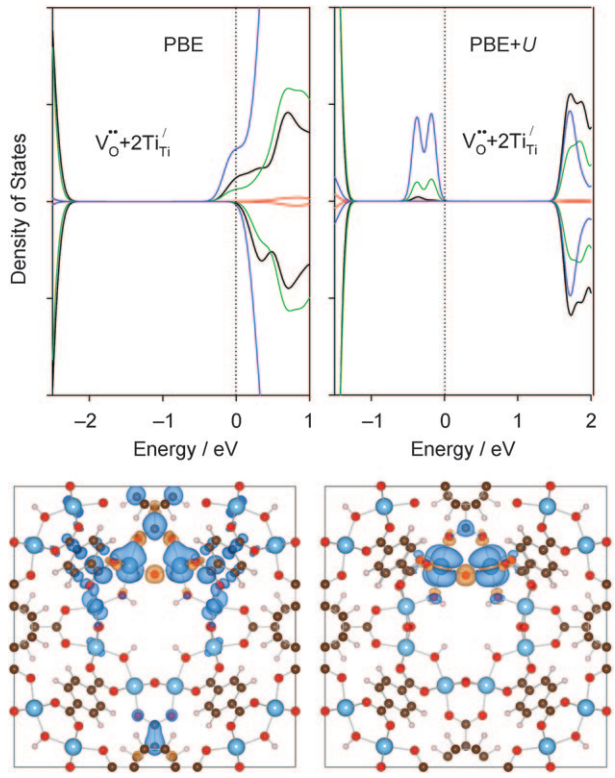

Figure 3. Electronic density of states and the density isosurface associated with the 16*n* oxygen vacancy in titanium carboxylate as calculated using the PBE and PBE + *U* density functionals, with the highest occupied state set to 0 eV. For the latter method, the defect state is more localized, resulting in a distinct split-off peak in the band gap.

Table 2. Calculated oxygen vacancy and hydroxyl defect reaction energies [eV] at two levels of DFT.

Defect reaction	GGA	GGA + *U*
$2\,Ti_{Ti} + O_O^{16n} \rightleftharpoons V_O^{\bullet\bullet} + 2\,Ti_{Ti}^{/} + \frac{1}{2}\,O_2$	3.66	2.72
$[O^{8h}H]_{OH} \rightleftharpoons H_{OH}^{x} + \frac{1}{2}\,O_2$	3.90	3.88
$[C{-}O^{16l}{-}Ti]^{x} \rightleftharpoons [C{-}Ti]^{x} + \frac{1}{2}\,O_2$	4.66	4.41
$Ti_{Ti} + O_O^{16n} + \frac{1}{2}\,H_2 \rightleftharpoons [OH]_O^{\bullet} + Ti_{Ti}^{/}$	−0.33	−0.64

tion is similar to that of oxygen vacancy formation, with localization of the excess electron on *one* of the neighbouring Ti sites, giving a local magnetic moment of 1 μ_B. A similar response has been identified on hydroxylation of the rutile TiO_2 (110) surface.[21] Equal distribution of the charge on the *two* neighbouring Ti sites results in a metastable configuration more than 0.5 eV higher in energy.

Due to the low defect reaction energies, optical excitations larger than the band gap ($h\nu > E_g$) will have sufficient energy to drive forward chemical reduction, which explains the facile photochromic behaviour. Specifically, in the hybrid material system, absorption of light across the band gap will generate an electron-hole pair localized in the titania and aromatic sublattices, respectively. The reduced Ti^{III} species are chemically stable; the appearance of a localized defect state near the centre of the band gap is consistent with the appearance of new visible absorption features after UV irradiation, which correspond to transitions between the defect state and the valence and conduction bands. The generated hole may be transferred to a sacrificial reagent such as an alcohol group,[12] or may facilitate the oxidation of the inorganic sublattice to release gaseous oxygen. While a high order theoretical approach, such as self-consistent *GW*, would remove the empiricism in the chosen value of *U*, we expect that this fundamental conclusion would remain unchanged.

In addition to the demonstrated photochromic behaviour, the spatial separation of electrons and holes is highly desirable for photovoltaic applications,[22] and our results demonstrate that this feature, an intrinsic type-II heterojunction, can be incorporated into hybrid organic-inorganic materials. A key goal in the future will be to engineer this characteristic into lower band gap hybrid materials, such as lead chalcogenides,[11] which can then absorb a significant fraction of the terrestrial solar spectrum for light harvesting applications.

In conclusion, examination of the electronic and defect structure of a novel hybrid titania material has confirmed the spatial separation of electrons and holes between the inorganic and organic sub-networks. Chemical reduction of Ti^{IV} to Ti^{III} can be readily achieved through intrinsic defect formation (oxygen loss) or through extrinsic reductants (e.g. H_2). The remarkably low energy for these processes, which is less than those in bulk TiO_2 and below the band gap energy, explains the facile colour change of this material after irradiation under UV light: photostimulated chemical reduction. These results suggest that immense potential exists in tailoring the properties of hybrid materials for photochemical applications.

Acknowledgements

A.W. would like to acknowledge funding from a Marie-Curie Intra-European Fellowship from the European Union under the Seventh Framework Programme. Via our membership of the UK's HPC Materials Chemistry Consortium, which is funded by EPSRC (EP/F067496), this work made use of the facilities of HECToR, the UK's national high-performance computing service.

Keywords: hybrid materials · metal–organic frameworks · photochemistry · reduction · titanium

[1] A. L. Linsebigler, G. Lu, J. T. Yates, *Chem. Rev.* **1995**, *95*, 735.
[2] A. Fujishima, K. Honda, *Nature* **1972**, *238*, 37.
[3] A. Fujishima, K. Honda, *Bull. Chem. Soc. Jpn.* **1971**, *44*, 1148.
[4] B. J. Morgan, D. O. Scanlon, G. W. Watson, *J. Mater. Chem.* **2009**, *19*, 5175 – 5178.
[5] Y. Gai, J. Li, S.-S. Li, J.-B. Xia, S.-H. Wei, *Phys. Rev. Lett.* **2009**, *102*, 036402 – 036404.
[6] M. Grätzel, *Nature* **2001**, *414*, 338 – 344.
[7] M. Grätzel, *Prog. Photovoltaics.* **2000**, *8*, 171.
[8] A. K. Cheetham, C. N. R. Rao, *Science* **2007**, *318*, 58 – 59.
[9] A. K. Cheetham, C. N. R. Rao, R. K. Feller, *Chem. Commun.* **2006**, 4780.
[10] G. Férey, *Chem. Mater.* **2001**, *13*, 3084.
[11] A. Walsh, *J. Phys. Chem. Lett.* **2010**, *1*, 1284 – 1287.
[12] M. Dan-Hardi, C. Serre, T. Frot, L. Rozes, G. Maurin, C. Sanchez, G. Ferey, *J. Am. Chem. Soc.* **2009**, *131*, 10857.
[13] C. Di Valentin, G. Pacchioni, A. Selloni, *J. Phys. Chem. C* **2009**, *113*, 20543.
[14] B. J. Morgan, G. W. Watson, *Phys. Rev. B* **2009**, *80*, 233102.

 © 2010 Wiley-VCH Verlag GmbH & Co. KGaA, Weinheim

[15] G. Kresse, J. Furthmüller, *Phys. Rev. B* **1996**, *54*, 11169.
[16] G. Kresse, J. Furthmüller, *Comput. Mater. Sci.* **1996**, *6*, 15.
[17] J. P. Perdew, K. Burke, M. Ernzerhof, *Phys. Rev. Lett.* **1996**, *77*, 3865.
[18] S. L. Dudarev, G. A. Botton, S. Y. Savrasov, C. J. Humphreys, A. P. Sutton, *Phys. Rev. B* **1998**, *57*, 1505.
[19] H. J. Monkhorst, J. D. Pack, *Phys. Rev. B* **1976**, *13*, 5188.
[20] B. J. Morgan, G. W. Watson, *Surf. Sci.* **2007**, *601*, 5034.
[21] C. Di Valentin, G. Pacchioni, A. Selloni, *Phys. Rev. Lett.* **2006**, *97*, 166803.
[22] C. Tao, J. Sun, X. Zhang, R. Yamachika, D. Wegner, Y. Bahri, G. Samsonidze, M. L. Cohen, S. G. Louie, T. D. Tilley, R. A. Segalman, M. F. Crommie, *Nano Lett.* **2009**, *9*, 3963.

Received: April 15, 2010
Published online on June 30, 2010

 © 2010 Wiley-VCH Verlag GmbH & Co. KGaA, Weinheim